

Characterizing dynamical criticality of many-body localization transitions from the Fock-space perspective

Zheng-Hang Sun,¹ Yong-Yi Wang,^{2,3,*} Jian Cui,^{4,†} Heng Fan,^{2,3,5,6,7,‡} and Markus Heyl¹

¹*Theoretical Physics III, Center for Electronic Correlations and Magnetism, Institute of Physics, University of Augsburg, D-86135 Augsburg, Germany*

²*Institute of Physics, Chinese Academy of Sciences, Beijing 100190, China*

³*School of Physical Sciences, University of Chinese Academy of Sciences, Beijing 100190, China*

⁴*School of Physics, Beihang University, Beijing 100191, China*

⁵*Songshan Lake Materials Laboratory, Dongguan 523808, Guangdong, China*

⁶*Beijing Academy of Quantum Information Sciences, Beijing 100193, China*

⁷*Hefei National Laboratory, Hefei 230088, China*

Characterizing the nature of many-body localization transitions (MBLTs) and their potential critical behaviors has remained a challenging problem. In this work, we study the dynamics of the displacement, quantifying the spread of the radial probability distribution in the Fock space, for systems with MBLTs, and perform a finite-size scaling analysis. We find that the scaling exponents satisfy theoretical bounds, and can identify universality classes. We show that reliable extrapolations to the thermodynamic limit for the MBLT induced by quasiperiodic fields is possible even for computationally accessible system sizes. Our work highlights that the displacement is a valuable tool for studying MBLTs, as relevant to ongoing experimental efforts.

The study of non-equilibrium phases and phase transitions of many-body quantum systems is a central focus in modern physics [1]. In particular, in disordered systems a paradigmatic non-equilibrium phase transition is expected to occur from an ergodic to the many-body localized (MBL) phase upon increasing the disorder strength, known as the many-body localization transition (MBLT) [2–19]. Although the phenomenology of the deep MBL phase based on the local integrals of motions has made substantial progress [20, 21], precisely characterizing the critical properties of MBLTs, such as the location of transition points and their universality classes, has remained an outstanding challenge [6].

One general method for identifying critical properties of continuous phase transitions is to study a data collapse with a subsequent finite-size scaling analysis. In the context of MBL, this is typically based on the properties of highly-excited eigenstates and eigenvalues obtained from exact diagonalization (ED) calculations, with the level-spacing ratio as a prominent example [17, 18, 22–29]. However, the scaling exponent ν obtained in this way usually violates some general bounds, such as the Harris-Chayes bound $\nu > 2$ for the MBLT in one-dimensional (1D) systems induced by random fields [30–32]. An alternative way to study MBLTs is to focus on the dynamics of local observables, such as the imbalance, which is of key importance due to its experimental relevance [33–39]. However, it has been pointed out that there is an obvious discrepancy between the transition points estimated by using the level-spacing ratio and those characterized by the freezing dynamics of imbalance, as another widely adopted landmark of MBLTs [40–43].

Recent developments highlight the suitability to characterize MBLTs upon studying the quantum states in the Fock

space. In particular, this includes the so-called radial distribution measuring the probability $\Pi(x)$ for an initially localized wave packet in Fock space to delocalize over a distance x [44–52]. Importantly, it has been shown that the distribution becomes distinctively broad in the vicinity of the MBLTs [50, 51]. In addition to the theoretical studies, it is worthwhile to note a recent experiment where the Fock-space dynamics in a disordered superconducting circuit has been measured, showing that the radial distribution can be experimentally feasible probes for signaling MBLTs [53]. Although there has been both theoretical and experimental progress in understanding MBLTs from the Fock-space perspective, a detailed and comprehensive finite-size scaling analysis, which plays a key role in characterizing precise critical properties of quantum phase transitions [54], of the radial distribution has remained absent so far.

In this work, we show that the width of the radial probability distribution, the so-called displacement, turns out to be a suitable quantity to characterize MBLTs through data collapse and finite-size scaling analysis. Specifically, we find reliable estimates of the critical points of MBLTs and scaling exponents, which satisfy the aforementioned theoretical bounds. We further discuss the possibility to perform extrapolations of the results obtained from the displacement to the limit of infinite system size. We observe that among three paradigmatic model systems, the MBLT in a Heisenberg chain with quasiperiodic disorder admits a most consistent scaling analysis and reliable extrapolation to the thermodynamic limit. Our work opens the door to also experimentally identify the dynamical phase diagram and universality classes of MBLTs using large-scale analog quantum simulations with the potential to overcome the numerical limitations from finite-size effects.

Models and probes.— We focus on three models including the 1D spin-1/2 Heisenberg model with random as well as quasiperiodic field, and a Floquet random-circuit model for the MBLT [55, 56]. Let us first introduce the considered

* yywang@iphy.ac.cn

† jianCui@buaa.edu.cn

‡ hfan@iphy.ac.cn

Heisenberg model:

$$\hat{H} = \hat{H}_{XY} + \hat{H}_{ZZ} + \hat{H}_Z, \quad (1)$$

where $\hat{H}_{XY} = J \sum_{r=1,2} \sum_{j=1}^{L-r} (\hat{S}_j^x \hat{S}_{j+r}^x + \hat{S}_j^y \hat{S}_{j+r}^y)$, $\hat{H}_{ZZ} = J \sum_{j=1}^{L-1} \hat{S}_j^z \hat{S}_{j+1}^z$, with J being the coupling strength, and $\hat{H}_Z = W \sum_{j=1}^L \cos(2\pi k j + \phi_j) \hat{S}_j^z$ describing the on-site disordered fields with the strength W , and $k = (\sqrt{5} - 1)/2$. For the quasiperiodic and random model, we consider the global phase offset $\phi_j = \phi \in [0, 2\pi)$ for all $j = 1, 2, \dots, L$, and the ϕ_j randomly drawn from a uniform distribution $[0, 2\pi)$, respectively. For the Hamiltonian (1), the location of critical points estimated by the ED calculations of the level spacing ratio is $W^{(r)} \simeq 4.3$ and 5.5 for the quasiperiodic and random model, respectively [15]. Moreover, both the numerical works based on the ED [15] and the renormalization group [16] indicate that the MBLTs in random and quasiperiodic systems belong to two different universality classes.

In addition to Heisenberg models (1), whose dynamics has both the conservation of energy and $U(1)$ symmetry, we consider a Floquet model [56]

$$\hat{U}_F = \hat{U}_u \hat{U}_d, \quad (2)$$

where $\hat{U}_d = \otimes_{i=1}^L \hat{d}_i$ with \hat{d}_i being a single-qubit gate at i -th site, generated by sampling a 2×2 random matrix from the circular unitary ensemble and then diagonalizing it, and $\hat{U}_u = \otimes_{j=1}^{L-1} \exp[(i/W) \hat{M}_{k_j, k_{j+1}}]$ with $k_j \in S_{L-1}$ being a random permutation, $\hat{M}_{k_j, k_{j+1}}$ as a 4×4 random matrix sampled from the Gaussian unitary ensemble, and W as the effective disorder strength. The Floquet model is free of any conservation laws, eliminating the influence of conserved quantities on the physics of MBLTs. Recent work shows that the critical point of the MBLT in the Floquet model (2) estimated by the level spacing ratio is $W^{(r)} \simeq 6$, while based on the resonance properties, the critical point satisfies $W_c > 13$ [56].

We now introduce the radial probability distribution defined in the Fock space. Consider a quantum many-body state $|\psi\rangle$, which can be chosen as a highly-excited eigenstate of a disordered model [50, 51], or a non-equilibrium state generated through time evolution [57, 58]. Then, the radial probability distribution $\Pi(x)$ can be defined as $\Pi(x) = \sum_{D_{Z, Z^*} = x} |\langle Z|\psi\rangle|^2$, where $|Z\rangle$ represents the product states in z -basis, i.e., $|Z\rangle = \otimes_{j=1}^L |z_j\rangle$ with $z_j \in \{-1, +1\}$ corresponding to the eigenstate of σ_j^z with the eigenvalue -1 and $+1$ [see Supplementary Materials for more details of $\Pi(x)$]. Here, D_{Z, Z^*} refers to the Hamming distance between the state $|Z\rangle$ and $|Z^*\rangle$, where $|Z^*\rangle$ labels the closest Fock state to $|\psi\rangle$, i.e., obtained through $\max_{Z'} |\langle Z'|\psi\rangle|^2 = |\langle Z^*|\psi\rangle|^2$. The spread of the radial probability distribution can be characterized by defining the moments $\bar{X}^n = \sum_x x^n \Pi(x)$, and the displacement

$$\Delta X^2 = \bar{X}^2 - (\bar{X})^2. \quad (3)$$

It has been shown that the quantity ΔX^2 exhibits a peak near the MBLT [50, 51].

For what follows we will adopt a non-equilibrium dynamical setting in close analogy to the capabilities in analog quan-

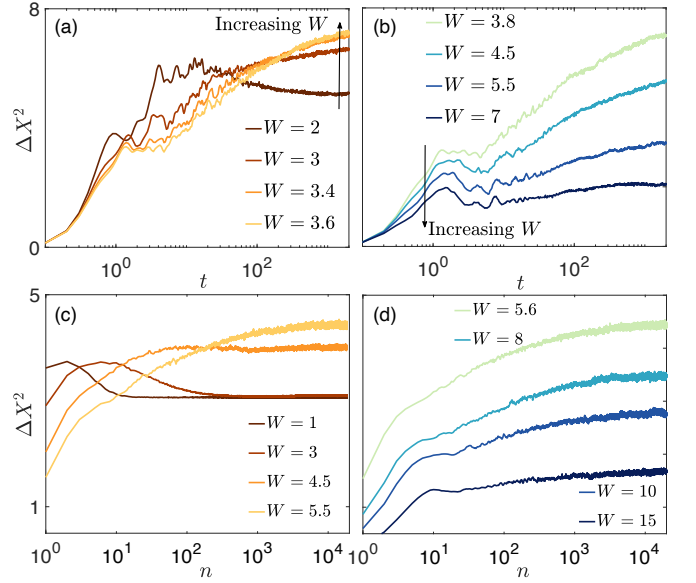


FIG. 1. (a) Time evolution of the displacement ΔX^2 for the Hamiltonian (1) with quasiperiodic fields and different disorder strengths W . (b) is similar to (a) but for larger W . In (a) and (b), the time t is in units where the coupling strength $J = 1$. (c) is similar to (a) but for the Floquet model (2). (d) is similar to (c) but for larger W .

tum simulation devices [53]. Concretely, we study the time-dependent state $|\psi(t)\rangle = \exp(-i\hat{H}t)|Z_0\rangle$ for the Hamiltonian systems whereas $|\psi(n)\rangle = \hat{U}_F^n|Z_0\rangle$ for the Floquet model. As initial state we choose the Néel state $|Z_0\rangle = \otimes_{j=1}^L |z_j\rangle$ with $z_j = (-1)^{j+1}$. In order to characterize the dynamics we mainly focus on the displacement ΔX^2 in what follows. We simulate the Hamiltonian dynamics by using Krylov subspace methods [59], whereas the Floquet model \hat{U}_F is solved by employing exact numerical simulation. The largest sizes for the Heisenberg models (1) and the Floquet model (2) are $L = 22$ and $L = 18$, respectively, with Hilbert space dimensions on the order of 10^5 . We employ at least 300 realizations for the disorder averaging for each system size L .

Dynamics.— We first consider the Heisenberg model in Eq. (1) with quasiperiodic fields. The results for different strengths of the field W at a system of size $L = 16$ are plotted in Fig. 1(a) and (b). In the ergodic phase ($W = 2$), after an initial increase and some intermediate drop, as a non-monotonic behavior, the displacement ΔX^2 finally approaches to a static value on the displayed time scales. For larger values of the disorder $W > 2$, ΔX^2 monotonically increases during the time evolution. More importantly, according to the results in Fig. 1(a) and (b), it is seen that the late-time value of ΔX^2 exhibits a peak around $W^* \simeq 3.6$ for the system of size $L = 16$, which is similar to the properties of the displacement ΔX^2 for highly-excited eigenstates [50, 51]. We also simulate the dynamics of ΔX^2 for the Floquet model in Eq. (2). As shown in Fig. 1(c) and (d), the dynamical behaviors of ΔX^2 are similar to those in the Heisenberg model (1).

Next, we determine the dynamics of ΔX^2 for the Heisenberg model (1) at different system sizes and an intermediate

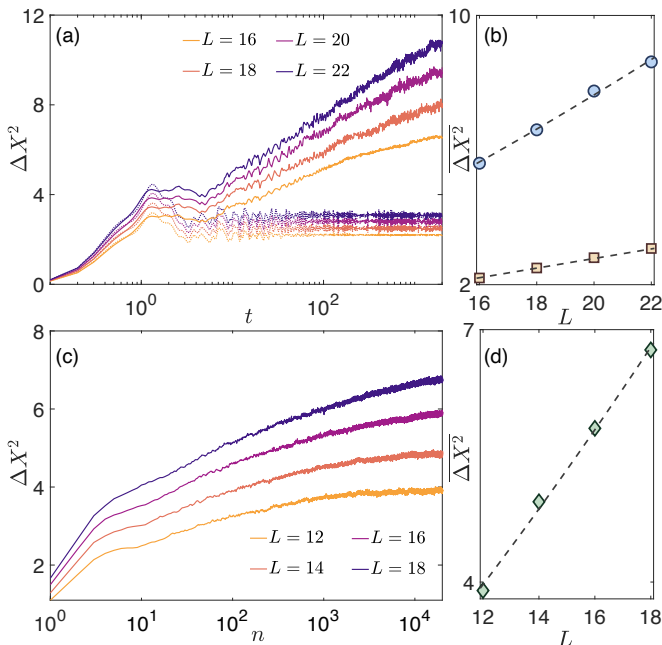


FIG. 2. (a) The solid (dotted) lines represent the time evolution of ΔX^2 for the Hamiltonian (1) (non-interacting model \hat{H}') with a strength $W = 4.1$ and different system sizes. The time t is in units where the coupling strength $J = 1$. (b) The time-averaged ΔX^2 , i.e., $\overline{\Delta X^2}$, as a function of L with the time interval $t \in [10, 1000]$. The circle and square data correspond to the interacting model with the Hamiltonian (1) and the non-interacting one \hat{H}' , respectively. (c) The time-evolution of ΔX^2 for the Floquet model (2) with the disorder strength $W = 7$ and different system sizes. (d) The $\overline{\Delta X^2}$ as a function of L for the Floquet model with the time interval $n \in [10^4, 2 \times 10^4]$. The dashed lines in (b) and (d) show the power-law fittings $\Delta X^2 \propto L^\beta$.

quasiperiodic-field strength $W = 4.1$. In order to highlight the effect of interactions we also consider a non-interacting model $\hat{H}' = \sum_{j=1}^{L-1} (\hat{S}_j^x \hat{S}_{j+1}^x + \hat{S}_j^y \hat{S}_{j+1}^y) + \hat{H}_Z$ with quasiperiodic fields, i.e., $\phi_j = \phi \in [0, 2\pi)$ in H_Z , where a transition between the extended phase and Anderson localization (AL) occurs at $W_c = 2$ [60]. As shown in Fig. 2(a), the dynamical behaviors of ΔX^2 for the interacting system are distinct from the non-interacting AL. For the AL, after a short-time increase, ΔX^2 saturates to relatively small values. In contrast, for the interacting case, there is an approximately logarithmic growth of the ΔX^2 . Theoretical studies indicate that near the critical point of the MBLT, ΔX^2 satisfies $\Delta X^2 \sim L^\beta$ with $1 < \beta \leq 2$ [50, 51]. By fitting the time-averaged ΔX^2 , defined as $\overline{\Delta X^2} = [\int_{t_i}^{t_f} dt \Delta X^2(t)](t_f - t_i)$ with the time interval $t \in [t_i, t_f]$, in Fig. 2(b), we show that $\overline{\Delta X^2} \sim L^{1.36}$ for the interacting case, while for the AL, $\overline{\Delta X^2} \sim L^{1.06}$ with an approximately linear size dependence. Moreover, for the Floquet model (2), an approximately logarithmic growth of the ΔX^2 can also be observed [see Fig. 2(c)]. In Fig. 2(d), we plot the time-averaged ΔX^2 as a function of system size L , showing that $\overline{\Delta X^2} \sim L^{1.32}$. We note that the details of the logarithmic fittings for the dynamics of ΔX^2 , and the power-

law fittings for $\overline{\Delta X^2}$ as a function of L in Fig. 2 are presented in the Supplementary Materials.

Scaling analysis.— After studying the temporal properties of ΔX^2 , we will now focus on a scaling analysis of the time-averaged values of ΔX^2 , denoted as $\overline{\Delta X^2}$. We consider a late time interval $t \in [800, 1000]$ for the average with moderate finite-time effect (see Supplementary Materials). We plot the $\overline{\Delta X^2}$ for different sizes L of the quasiperiodic model in Fig. 3(a). One can see that with increasing L , the location of the peak W^* shifts to larger value. To determine the location W_c of the transition point for the MBLT in the quasiperiodic model, we perform a data collapse [61], see in Fig. 3(a). For that purpose we consider the following form of the scaling function

$$\overline{\Delta X^2}(L, W) = L^\lambda g[(W - W_c)L^{1/\nu}], \quad (4)$$

which is based on the assumption of a divergent correlation length. The power-law scaling (4) can efficiently capture the critical properties of AL transitions in high-dimensional systems [62–64], and is also widely employed in the study of MBLTs [15–18].

As shown in Fig. 3(b), the best data collapse is obtained when $W_c = 6.1 \pm 0.6$, $\nu = 1.4 \pm 0.4$, and $\lambda = 1.2 \pm 0.2$. The scaling exponent ν satisfies the Harris-Luck bound $\nu > 1$ for 1D quasiperiodic systems [65]. We also calculate the $\overline{\Delta X^2}$ for the random model with different disorder strengths W and system sizes L , and perform again a data collapse based on Eq. (4). The results are displayed in Fig. 3(c) and (d). For the random model, we find the best collapse for $W_c = 11.7 \pm 2.0$, $\nu = 3.8 \pm 0.5$, and $\lambda = 1.1 \pm 0.1$. Two marks are in order. First, the estimated scaling exponent for the random model satisfies the Harris-Chayes bound $\nu > 2$ [30–32], and the distinct difference of ν for the random and quasiperiodic models indicates that the MBLTs induced by random and quasiperiodic fields belong to two different universality classes. Second, for both the random and quasiperiodic model, the critical points W_c extracted from the scaling analysis of the data of $\overline{\Delta X^2}$ are larger than the $W^{(r)}$ estimated by using the level-spacing ratio [15]. In Supplementary Materials, we show that the freezing dynamics of imbalance is observed when $W \geq W_c$, while there are obvious signatures of power-law decay of imbalance with $W = W^{(r)}$, suggesting that the scaling analysis of $\overline{\Delta X^2}$ gives a better estimation of the critical points. For the Floquet model (2), we consider the time interval $n \in [10^4, 2 \times 10^4]$ for the average of ΔX^2 . By employing the form of scaling function in Eq. (4), we obtain the critical point $W_c = 14.6 \pm 1.8$, which agrees with that estimated by the analysis of resonances [56]. The scaling exponent $\nu = 3.4 \pm 0.7$ satisfies the Harris-Chayes bound [30–32], and the small difference between the ν for the MBLT in the Floquet model (2) and that for the random Heisenberg model indicates that the MBLTs in the two aforementioned models belong to the same universality class.

Let us now characterize the accuracy of the obtained data collapse by checking self-consistently the extrapolation to the thermodynamic limit. For that purpose, we consider the location of the maximum $\overline{\Delta X^2}$ after the data collapse [marked

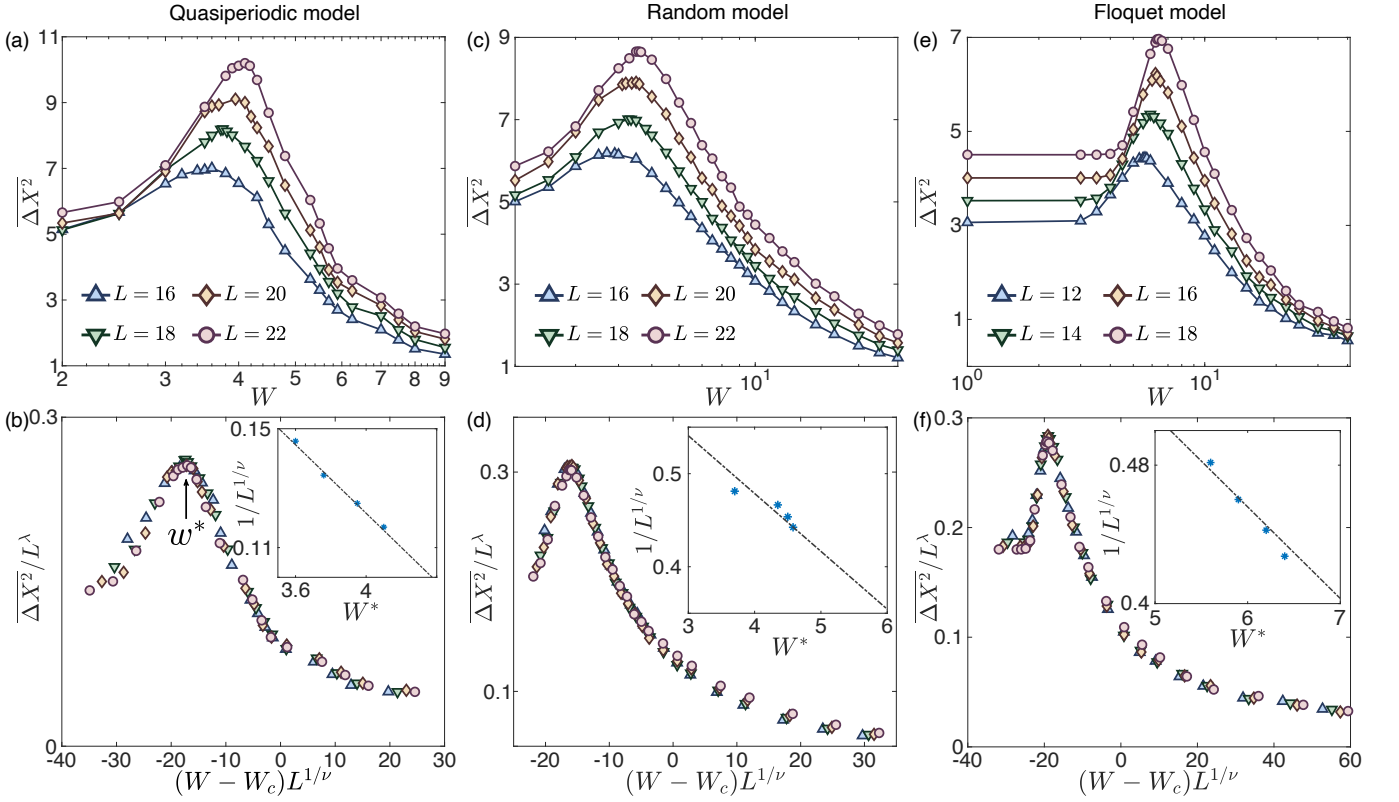


FIG. 3. (a) The value of $\overline{\Delta X^2}$ as a function of disorder strength W , for the quasiperiodic model with sizes $L = 16, 18, 20$ and 22 . (b) Finite-size data collapse for the data of $\overline{\Delta X^2}$ shown in (a), with $W_c = 6.1 \pm 0.6$, $\nu = 1.4 \pm 0.4$, and $\lambda = 1.2 \pm 0.2$. The arrow marks the location of maximum $\overline{\Delta X^2}$ after the data collapse, w^* , which is defined in Eq. (5). (c) is similar to (a) but for the random model. (d) Finite-size data collapse for the data of $\overline{\Delta X^2}$ shown in (c), with $W_c = 11.7 \pm 2.0$, $\nu = 3.8 \pm 0.5$, and $\lambda = 1.1 \pm 0.1$. (e) The value of $\overline{\Delta X^2}$ as a function of W , for the Floquet model with sizes $L = 12, 14, 16$ and 18 . (f) Finite-size data collapse for the data shown in (e), with $W_c = 14.6 \pm 1.8$, $\nu = 3.4 \pm 0.7$, and $\lambda = 1.1 \pm 0.1$. The marks in the inset of (b), (d) and (f) are the location of maximum $\overline{\Delta X^2}$, denoted as W^* , versus different system size with the ν obtained from the data collapse. The dashed line in the inset of (b), (d) and (f) represents Eq. (5) with the parameters ν , W_c and w^* obtained from the data collapse. The coefficient of determination R^2 for the marks and the dashed line in inset of (b), (d) and (f) are 0.99, 0.54 and 0.95, respectively.

in Fig. 3(b) as an example] as $w^* = (W^* - W_c)L^{1/\nu}$, where W^* is the maximum point *before* the data collapse for each L . This suggests that

$$\frac{1}{L^{1/\nu}} = \frac{W^*}{w^*} - \frac{W_c}{w^*}. \quad (5)$$

In the inset of Fig. 3(b), (d) and (f), we plot W^* versus $1/L^{1/\nu}$, and the linear function (5) with the parameters ν , W_c and w^* obtained from the data collapse. As shown in the inset of Fig. 3(d), for the random Heisenberg model, Eq. (5) does not align well the data of W^* . This indicates a stronger finite-size effect of the MBLT induced by random fields, which may be due to the presence of rare thermal regions in the random model, resulting in the instability of the MBLT [66–70]. In contrast, the rare thermal regions are absent for the quasiperiodic model, which may be the reason for the stability of the MBLTs induced by quasiperiodic fields, consistent with the well alignment of Eq. (5) shown in the inset of Fig. 3(b). Moreover, in comparison with the random Heisenberg model, the MBLT in the Floquet model (2) is more stable, which agrees with a recent study revealing moderate finite-size ef-

fects for the MBLTs in disordered Floquet systems [18].

Summary and discussions.— In our work we show that the critical properties of MBLTs can be characterized through a data collapse of the displacement ΔX^2 and a subsequent finite-size scaling analysis. Our results suggest that critical properties of the MBLT induced by the quasiperiodic fields can be well captured by the scaling analysis, while for the MBLTs in the model with random fields and the Floquet model, finite-size effects are stronger for the numerically accessible system sizes.

Given that the non-equilibrium dynamics of ΔX^2 can be efficiently measured in analog quantum simulations [53], a future perspective of our work is to experimentally study MBLTs by using the data collapse and scaling analysis in large-scale quantum simulators, which can overcome the finite-size effects of our present numerics. Moreover, our work paves the way of studying the MBLTs in more complex systems from the Fock space point of view, such as for two-dimensional systems [34, 71–73], systems with long-range interactions [44, 74–79], Bose/Fermi-Hubbard models [28, 80, 81], discrete time crystals protected by MBL [82–

85], and systems subjected to linear potentials exhibiting the Stark MBL [86–90].

ACKNOWLEDGMENTS

This work was supported by National Key Research and Development Program of China (Grant No. 2021YFA1402001), National Natural Science Foun-

dation of China (Grants Nos. 92265207, T2121001, 11934018, 12375007), Innovation Program for Quantum Science and Technology (Grant No. 2-6), Beijing Natural Science Foundation (Grant No. Z200009), Scientific Instrument Developing Project of Chinese Academy of Sciences (Grant No. YJKYYQ20200041), the European Research Council (ERC) under the European Union’s Horizon 2020 research and innovation programme (grant agreement No. 853443), and the German Research Foundation DFG via project 499180199 (FOR 5522).

-
- [1] J. Eisert, M. Friesdorf, and C. Gogolin, “Quantum many-body systems out of equilibrium,” *Nature Physics* **11**, 124–130 (2015).
- [2] Rahul Nandkishore and David A. Huse, “Many-body localization and thermalization in quantum statistical mechanics,” *Annual Review of Condensed Matter Physics* **6**, 15–38 (2015).
- [3] Dmitry A. Abanin and Zlatko Papić, “Recent progress in many-body localization,” *Annalen der Physik* **529**, 1700169 (2017).
- [4] Ehud Altman, “Many-body localization and quantum thermalization,” *Nature Physics* **14**, 979–983 (2018).
- [5] Dmitry A. Abanin, Ehud Altman, Immanuel Bloch, and Maksym Serbyn, “Colloquium: Many-body localization, thermalization, and entanglement,” *Reviews of Modern Physics* **91**, 021001– (2019).
- [6] Piotr Sierant, Maciej Lewenstein, Antonello Scardicchio, Lev Vidmar, and Jakub Zakrzewski, “Many-Body Localization in the Age of Classical Computing,” *arXiv e-prints*, arXiv:2403.07111 (2024), arXiv:2403.07111 [cond-mat.dis-nn].
- [7] Arijeet Pal and David A. Huse, “Many-body localization phase transition,” *Phys. Rev. B* **82**, 174411 (2010).
- [8] Trithev Devakul and Rajiv R. P. Singh, “Early breakdown of area-law entanglement at the many-body delocalization transition,” *Phys. Rev. Lett.* **115**, 187201 (2015).
- [9] Maksym Serbyn, Z. Papić, and Dmitry A. Abanin, “Criterion for many-body localization-delocalization phase transition,” *Phys. Rev. X* **5**, 041047 (2015).
- [10] Andrew C. Potter, Romain Vasseur, and S. A. Parameswaran, “Universal properties of many-body delocalization transitions,” *Phys. Rev. X* **5**, 031033 (2015).
- [11] Ronen Vosk, David A. Huse, and Ehud Altman, “Theory of the many-body localization transition in one-dimensional systems,” *Phys. Rev. X* **5**, 031032 (2015).
- [12] Vedika Khemani, S. P. Lim, D. N. Sheng, and David A. Huse, “Critical properties of the many-body localization transition,” *Phys. Rev. X* **7**, 021013 (2017).
- [13] Philipp T. Dumitrescu, Romain Vasseur, and Andrew C. Potter, “Scaling theory of entanglement at the many-body localization transition,” *Phys. Rev. Lett.* **119**, 110604 (2017).
- [14] Nicolas Macé, Fabien Alet, and Nicolas Laflorencie, “Multifractal scalings across the many-body localization transition,” *Phys. Rev. Lett.* **123**, 180601 (2019).
- [15] Vedika Khemani, D. N. Sheng, and David A. Huse, “Two universality classes for the many-body localization transition,” *Phys. Rev. Lett.* **119**, 075702 (2017).
- [16] Shi-Xin Zhang and Hong Yao, “Universal properties of many-body localization transitions in quasiperiodic systems,” *Phys. Rev. Lett.* **121**, 206601 (2018).
- [17] David J. Luitz, Nicolas Laflorencie, and Fabien Alet, “Many-body localization edge in the random-field heisenberg chain,” *Phys. Rev. B* **91**, 081103 (2015).
- [18] Piotr Sierant, Maciej Lewenstein, Antonello Scardicchio, and Jakub Zakrzewski, “Stability of many-body localization in floquet systems,” *Phys. Rev. B* **107**, 115132 (2023).
- [19] Matthew Rispoli, Alexander Lukin, Robert Schittko, Sooshin Kim, M. Eric Tai, Julian Léonard, and Markus Greiner, “Quantum critical behaviour at the many-body localization transition,” *Nature* **573**, 385–389 (2019).
- [20] David A. Huse, Rahul Nandkishore, and Vadim Oganesyan, “Phenomenology of fully many-body-localized systems,” *Phys. Rev. B* **90**, 174202 (2014).
- [21] Maksym Serbyn, Z. Papić, and Dmitry A. Abanin, “Local conservation laws and the structure of the many-body localized states,” *Phys. Rev. Lett.* **111**, 127201 (2013).
- [22] Vadim Oganesyan and David A. Huse, “Localization of interacting fermions at high temperature,” *Phys. Rev. B* **75**, 155111 (2007).
- [23] Elliott Baygan, S. P. Lim, and D. N. Sheng, “Many-body localization and mobility edge in a disordered spin- $\frac{1}{2}$ heisenberg ladder,” *Phys. Rev. B* **92**, 195153 (2015).
- [24] Mac Lee, Thomas R. Look, S. P. Lim, and D. N. Sheng, “Many-body localization in spin chain systems with quasiperiodic fields,” *Phys. Rev. B* **96**, 075146 (2017).
- [25] Kazue Kudo and Tetsuo Deguchi, “Finite-size scaling with respect to interaction and disorder strength at the many-body localization transition,” *Phys. Rev. B* **97**, 220201 (2018).
- [26] Johnnie Gray, Sougato Bose, and Abolfazl Bayat, “Many-body localization transition: Schmidt gap, entanglement length, and scaling,” *Phys. Rev. B* **97**, 201105 (2018).
- [27] Dariusz Wiater and Jakub Zakrzewski, “Impact of geometry on many-body localization,” *Phys. Rev. B* **98**, 094202 (2018).
- [28] Tuure Orell, Alexios A. Michailidis, Maksym Serbyn, and Matti Silveri, “Probing the many-body localization phase transition with superconducting circuits,” *Phys. Rev. B* **100**, 134504 (2019).
- [29] Jan Šuntajs, Janez Bonča, Tomaž Prosen, and Lev Vidmar, “Ergodicity breaking transition in finite disordered spin chains,” *Phys. Rev. B* **102**, 064207 (2020).
- [30] A B Harris, “Effect of random defects on the critical behaviour of ising models,” *Journal of Physics C: Solid State Physics* **7**, 1671 (1974).
- [31] J. T. Chayes, L. Chayes, Daniel S. Fisher, and T. Spencer, “Finite-size scaling and correlation lengths for disordered systems,” *Phys. Rev. Lett.* **57**, 2999–3002 (1986).
- [32] A. Chandran, C. R. Laumann, and V. Oganesyan, “Finite size scaling bounds on many-body localized phase transitions,” (2015), arXiv:1509.04285 [cond-mat.dis-nn].
- [33] Michael Schreiber, Sean S. Hodgman, Pranjal Bordia, Henrik P.

- Lüschen, Mark H. Fischer, Ronen Vosk, Ehud Altman, Ulrich Schneider, and Immanuel Bloch, "Observation of many-body localization of interacting fermions in a quasirandom optical lattice," *Science* **349**, 842–845 (2015).
- [34] Jae-yoon Choi, Sebastian Hild, Johannes Zeiher, Peter Schauß, Antonio Rubio-Abadal, Tarik Yefsah, Vedika Khemani, David A. Huse, Immanuel Bloch, and Christian Gross, "Exploring the many-body localization transition in two dimensions," *Science* **352**, 1547–1552 (2016).
- [35] J. Smith, A. Lee, P. Richerme, B. Neyenhuis, P. W. Hess, P. Hauke, M. Heyl, D. A. Huse, and C. Monroe, "Many-body localization in a quantum simulator with programmable random disorder," *Nature Physics* **12**, 907–911 (2016).
- [36] Henrik P. Lüschen, Pranjal Bordia, Sebastian Scherg, Fabien Alet, Ehud Altman, Ulrich Schneider, and Immanuel Bloch, "Observation of slow dynamics near the many-body localization transition in one-dimensional quasiperiodic systems," *Phys. Rev. Lett.* **119**, 260401 (2017).
- [37] Pranjal Bordia, Henrik Lüschen, Sebastian Scherg, Sarang Gopalakrishnan, Michael Knap, Ulrich Schneider, and Immanuel Bloch, "Probing slow relaxation and many-body localization in two-dimensional quasiperiodic systems," *Phys. Rev. X* **7**, 041047 (2017).
- [38] B. Chiaro, C. Neill, A. Bohrdt, M. Filippone, F. Arute, K. Arya, R. Babbush, D. Bacon, J. Bardin, R. Barends, S. Boixo, D. Buell, B. Burkett, Y. Chen, Z. Chen, R. Collins, A. Dunsworth, E. Farhi, A. Fowler, B. Foxen, C. Gidney, M. Giustina, M. Harrigan, T. Huang, S. Isakov, E. Jeffrey, Z. Jiang, D. Kafri, K. Kechedzhi, J. Kelly, P. Klimov, A. Korotkov, F. Kostritsa, D. Landhuis, E. Lucero, J. McClean, X. Mi, A. Megrant, M. Mohseni, J. Mutus, M. McEwen, O. Naaman, M. Neeley, M. Niu, A. Petukhov, C. Quintana, N. Rubin, D. Sank, K. Satzinger, T. White, Z. Yao, P. Yeh, A. Zalcman, V. Smelyanskiy, H. Neven, S. Gopalakrishnan, D. Abanin, M. Knap, J. Martinis, and P. Roushan, "Direct measurement of nonlocal interactions in the many-body localized phase," *Phys. Rev. Res.* **4**, 013148 (2022).
- [39] Qiujiang Guo, Chen Cheng, Zheng-Hang Sun, Zixuan Song, Hekang Li, Zhen Wang, Wenhui Ren, Hang Dong, Dongning Zheng, Yu-Ran Zhang, Rubem Mondaini, Heng Fan, and H. Wang, "Observation of energy-resolved many-body localization," *Nature Physics* **17**, 234–239 (2021).
- [40] Elmer V. H. Doggen, Frank Schindler, Konstantin S. Tikhonov, Alexander D. Mirlin, Titus Neupert, Dmitry G. Polyakov, and Igor V. Gornyi, "Many-body localization and delocalization in large quantum chains," *Phys. Rev. B* **98**, 174202 (2018).
- [41] Elmer V. H. Doggen and Alexander D. Mirlin, "Many-body delocalization dynamics in long Aubry-André quasiperiodic chains," *Phys. Rev. B* **100**, 104203 (2019).
- [42] Titas Chanda, Piotr Sierant, and Jakub Zakrzewski, "Time dynamics with matrix product states: Many-body localization transition of large systems revisited," *Phys. Rev. B* **101**, 035148 (2020).
- [43] Piotr Sierant and Jakub Zakrzewski, "Challenges to observation of many-body localization," *Phys. Rev. B* **105**, 224203 (2022).
- [44] Philipp Hauke and Markus Heyl, "Many-body localization and quantum ergodicity in disordered long-range Ising models," *Phys. Rev. B* **92**, 134204 (2015).
- [45] Soumya Bera, Henning Schomerus, Fabian Heidrich-Meisner, and Jens H. Bardarson, "Many-body localization characterized from a one-particle perspective," *Phys. Rev. Lett.* **115**, 046603 (2015).
- [46] David E. Logan and Staszek Welsh, "Many-body localization in Fock space: A local perspective," *Phys. Rev. B* **99**, 045131 (2019).
- [47] Soumi Ghosh, Atithi Acharya, Subhayan Sahu, and Subroto Mukerjee, "Many-body localization due to correlated disorder in Fock space," *Phys. Rev. B* **99**, 165131 (2019).
- [48] Sthitadhi Roy and David E. Logan, "Fock-space correlations and the origins of many-body localization," *Phys. Rev. B* **101**, 134202 (2020).
- [49] Jagannath Sutradhar, Soumi Ghosh, Sthitadhi Roy, David E. Logan, Subroto Mukerjee, and Sumilan Banerjee, "Scaling of the Fock-space propagator and multifractality across the many-body localization transition," *Phys. Rev. B* **106**, 054203 (2022).
- [50] Sthitadhi Roy and David E. Logan, "Fock-space anatomy of eigenstates across the many-body localization transition," *Phys. Rev. B* **104**, 174201 (2021).
- [51] Giuseppe De Tomasi, Ivan M. Khaymovich, Frank Pollmann, and Simone Warzel, "Rare thermal bubbles at the many-body localization transition from the Fock space point of view," *Phys. Rev. B* **104**, 024202 (2021).
- [52] Soumi Ghosh, Jagannath Sutradhar, Subroto Mukerjee, and Sumilan Banerjee, "Scaling of Fock space propagator in quasiperiodic many-body localizing systems," *arXiv e-prints*, arXiv:2401.03027 (2024), arXiv:2401.03027 [cond-mat.dis-nn].
- [53] Yunyan Yao, Liang Xiang, Zexian Guo, Zehang Bao, Yong-Feng Yang, Zixuan Song, Haohai Shi, Xuhao Zhu, Feitong Jin, Jiachen Chen, Shibo Xu, Zitian Zhu, Fanhao Shen, Ning Wang, Chuanyu Zhang, Yaozu Wu, Yiren Zou, Pengfei Zhang, Hekang Li, Zhen Wang, Chao Song, Chen Cheng, Rubem Mondaini, H. Wang, J. Q. You, Shi-Yao Zhu, Lei Ying, and Qiujiang Guo, "Observation of many-body Fock space dynamics in two dimensions," *Nature Physics* (2023), 10.1038/s41567-023-02133-0.
- [54] John Cardy, *Scaling and Renormalization in Statistical Physics*, Cambridge Lecture Notes in Physics (Cambridge University Press, 1996).
- [55] Christoph Sünnderhauf, David Pérez-García, David A. Huse, Norbert Schuch, and J. Ignacio Cirac, "Localization with random time-periodic quantum circuits," *Phys. Rev. B* **98**, 134204 (2018).
- [56] Alan Morningstar, Luis Colmenarez, Vedika Khemani, David J. Luitz, and David A. Huse, "Avalanches and many-body resonances in many-body localized systems," *Phys. Rev. B* **105**, 174205 (2022).
- [57] Giuseppe De Tomasi, Daniel Hetterich, Pablo Sala, and Frank Pollmann, "Dynamics of strongly interacting systems: From Fock-space fragmentation to many-body localization," *Phys. Rev. B* **100**, 214313 (2019).
- [58] Isabel Creed, David E. Logan, and Sthitadhi Roy, "Probability transport on the Fock space of a disordered quantum spin chain," *Phys. Rev. B* **107**, 094206 (2023).
- [59] David J. Luitz and Yevgeny Bar Lev, "The ergodic side of the many-body localization transition," *Annalen der Physik* **529**, 1600350 (2017).
- [60] Serge Aubry and Gilles André, "Analyticity breaking and Anderson localization in incommensurate lattices," *Ann. Israel Phys. Soc.* **3**, 133 (1980).
- [61] Somendra M Bhattacharjee and Flavio Seno, "A measure of data collapse for scaling," *Journal of Physics A: Mathematical and General* **34**, 6375 (2001).
- [62] Matthias Lopez, Jean-François Clément, Pascal Szriftgiser, Jean-Claude Garreau, and Dominique Delande, "Experimental test of universality of the Anderson transition," *Phys. Rev. Lett.* **108**, 095701 (2012).
- [63] Keith Slevin and Tomi Ohtsuki, "Critical exponent for the Anderson transition in the three-dimensional orthogonal universal-

- ity class,” *New Journal of Physics* **16**, 015012 (2014).
- [64] M. Pino, “Scaling up the anderson transition in random-regular graphs,” *Phys. Rev. Res.* **2**, 042031 (2020).
- [65] J. M. Luck., “A classification of critical phenomena on quasicrystals and other aperiodic structures,” *Europhysics Letters* **24**, 359 (1993).
- [66] Wojciech De Roeck and Fran çois Huveneers, “Stability and instability towards delocalization in many-body localization systems,” *Phys. Rev. B* **95**, 155129 (2017).
- [67] David J. Luitz, Fran çois Huveneers, and Wojciech De Roeck, “How a small quantum bath can thermalize long localized chains,” *Phys. Rev. Lett.* **119**, 150602 (2017).
- [68] Thimothée Thiery, Fran çois Huveneers, Markus Müller, and Wojciech De Roeck, “Many-body delocalization as a quantum avalanche,” *Phys. Rev. Lett.* **121**, 140601 (2018).
- [69] P. J. D. Crowley and A. Chandran, “Avalanche induced coexisting localized and thermal regions in disordered chains,” *Phys. Rev. Res.* **2**, 033262 (2020).
- [70] Julian Léonard, Sooshin Kim, Matthew Rispoli, Alexander Lukin, Robert Schittko, Joyce Kwan, Eugene Demler, Dries Sels, and Markus Greiner, “Probing the onset of quantum avalanches in a many-body localized system,” *Nature Physics* **19**, 481–485 (2023).
- [71] Thorsten B. Wahl, Arijeet Pal, and Steven H. Simon, “Signatures of the many-body localized regime in two dimensions,” *Nature Physics* **15**, 164–169 (2019).
- [72] Elmer V. H. Doggen, Igor V. Gornyi, Alexander D. Mirlin, and Dmitry G. Polyakov, “Slow many-body delocalization beyond one dimension,” *Phys. Rev. Lett.* **125**, 155701 (2020).
- [73] K. S. C. Decker, D. M. Kennes, and C. Karrasch, “Many-body localization and the area law in two dimensions,” *Phys. Rev. B* **106**, L180201 (2022).
- [74] Alexander L. Burin, “Many-body delocalization in a strongly disordered system with long-range interactions: Finite-size scaling,” *Phys. Rev. B* **91**, 094202 (2015).
- [75] Rahul M. Nandkishore and S. L. Sondhi, “Many-body localization with long-range interactions,” *Phys. Rev. X* **7**, 041021 (2017).
- [76] A. Safavi-Naini, M. L. Wall, O. L. Acevedo, A. M. Rey, and R. M. Nandkishore, “Quantum dynamics of disordered spin chains with power-law interactions,” *Phys. Rev. A* **99**, 033610 (2019).
- [77] Sebastian Schiffer, Jia Wang, Xia-Ji Liu, and Hui Hu, “Many-body localization in xy spin chains with long-range interactions: An exact-diagonalization study,” *Phys. Rev. A* **100**, 063619 (2019).
- [78] Xiaolong Deng, Guido Masella, Guido Pupillo, and Luis Santos, “Universal algebraic growth of entanglement entropy in many-body localized systems with power-law interactions,” *Phys. Rev. Lett.* **125**, 010401 (2020).
- [79] Andrii O. Maksymov and Alexander L. Burin, “Many-body localization in spin chains with long-range transverse interactions: Scaling of critical disorder with system size,” *Phys. Rev. B* **101**, 024201 (2020).
- [80] Rubem Mondaini and Marcos Rigol, “Many-body localization and thermalization in disordered hubbard chains,” *Phys. Rev. A* **92**, 041601 (2015).
- [81] Piotr Sierant and Jakub Zakrzewski, “Many-body localization of bosons in optical lattices,” *New Journal of Physics* **20**, 043032 (2018).
- [82] N. Y. Yao, A. C. Potter, I.-D. Potirniche, and A. Vishwanath, “Discrete time crystals: Rigidity, criticality, and realizations,” *Phys. Rev. Lett.* **118**, 030401 (2017).
- [83] Dominic V. Else, Christopher Monroe, Chetan Nayak, and Norman Y. Yao, “Discrete time crystals,” *Annual Review of Condensed Matter Physics* **11**, 467–499 (2020).
- [84] Matteo Ippoliti, Kostyantyn Kechedzhi, Roderich Moessner, S.L. Sondhi, and Vedika Khemani, “Many-body physics in the nisq era: Quantum programming a discrete time crystal,” *PRX Quantum* **2**, 030346 (2021).
- [85] A. Kshetrimayum, M. Goihl, D. M. Kennes, and J. Eisert, “Quantum time crystals with programmable disorder in higher dimensions,” *Phys. Rev. B* **103**, 224205 (2021).
- [86] Evert van Nieuwenburg, Yuval Baum, and Gil Refael, “From bloch oscillations to many-body localization in clean interacting systems,” *Proceedings of the National Academy of Sciences* **116**, 9269–9274 (2019).
- [87] M. Schulz, C. A. Hooley, R. Moessner, and F. Pollmann, “Stark many-body localization,” *Phys. Rev. Lett.* **122**, 040606 (2019).
- [88] S. R. Taylor, M. Schulz, F. Pollmann, and R. Moessner, “Experimental probes of stark many-body localization,” *Phys. Rev. B* **102**, 054206 (2020).
- [89] Yong-Yi Wang, Zheng-Hang Sun, and Heng Fan, “Stark many-body localization transitions in superconducting circuits,” *Phys. Rev. B* **104**, 205122 (2021).
- [90] W. Morong, F. Liu, P. Becker, K. S. Collins, L. Feng, A. Kyprianidis, G. Pagano, T. You, A. V. Gorshkov, and C. Monroe, “Observation of stark many-body localization without disorder,” *Nature* **599**, 393–398 (2021).

Supplementary Material for “Characterizing dynamical criticality of many-body localization transitions from the Fock-space perspective”

Zheng-Hang Sun, Yong-Yi Wang, Jian Cui, Heng Fan, and Markus Heyl

I. FOCK-SPACE ANATOMY OF NON-EQUILIBRIUM STATES

In this section, we present more details of the Fock-space [see Fig. S1(a)] anatomy of non-equilibrium states. The first step is calculating the probabilities $P_Z = |\langle \psi | Z \rangle|^2$, with $|Z\rangle = \otimes_{j=1}^L |z_j\rangle$ ($z_j \in \{-1, +1\}$) being the product states in z -basis, and $|\psi\rangle$ being the non-equilibrium states we focus on. Next, we obtain the closest Fock state $|Z^*\rangle$ satisfying $\max_Z P_Z = P_{Z^*}$, and can calculate the Hamming distance x between an arbitrary state $|Z\rangle$ and the state $|Z^*\rangle$, i.e., D_{Z,Z^*} . We then can plot the radial probability distribution $\Pi(x) = \sum_{D_{Z,Z^*}=x} P_Z$, see Fig. S1(b) as an example for the Floquet model of many-body localization (MBL) with $L = 18$ and three different values of W . As shown in the Fig. 1(c) of the main text, with $W = 6.4$, there is a peak of the displacement $\Delta X^2 = \sum_x x^2 \Pi(x) - [\sum_x x \Pi(x)]^2$, corresponding to a broad distribution of $\Pi(x)$. We also display the probabilities P_Z for all the states $|Z\rangle$ in Fig. S1(c)-(e).

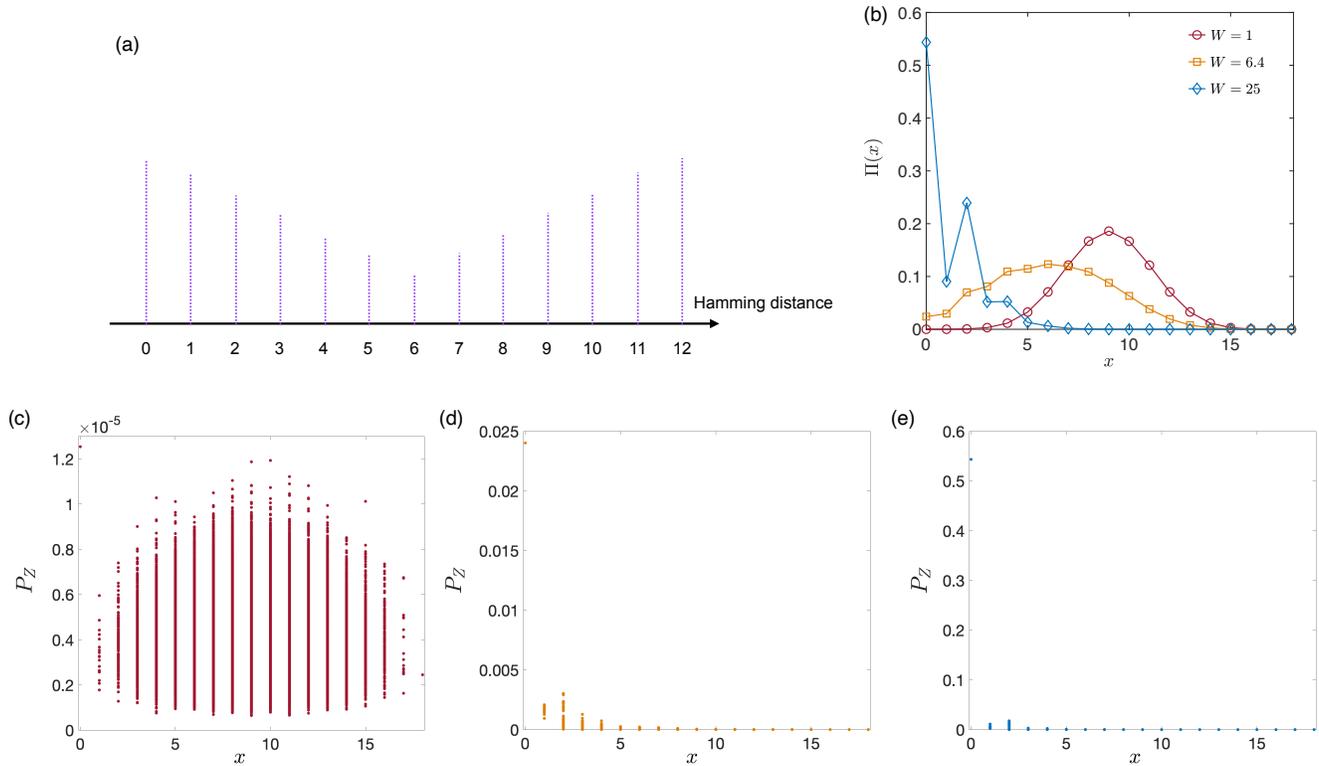


FIG. S1. (a) A schematic of the Fock space for the Floquet model of MBL as an example with size $L = 12$, where the 2^L pink nodes represent the z -basis vectors, classified by different Hamming distance. (b) The radial probability distribution $\Pi(x)$ versus the Hamming distance x for the non-equilibrium states $|\psi(n)\rangle$ obtained from the time evolution of the Floquet model with $n = 2 \times 10^4$ different values of W . (c) For the Floquet model with $W = 1$, the probabilities $P_Z = |\langle \psi(n) | Z \rangle|^2$, where $n = 2 \times 10^4$ and $|Z\rangle$ refers to the z -basis vectors, versus the Hamming distance x corresponding to the closest state $|Z^*\rangle$. (d) is similar to (c) but with $W = 6.4$. (e) is similar to (c) but with $W = 25$.

II. THE FINITE-TIME EFFECT

In this section, we present additional data for the time-averaged displacement $\overline{\Delta X^2} = \int_{t_i}^{t_f} dt \Delta X^2(t)$ with the time interval $t \in [t_i, t_f]$. In the main text, for the disordered Heisenberg model, we consider the time interval $t \in [800, 1000]$. Here, we calculate the $\overline{\Delta X^2}$ for the time intervals with longer time, i.e., $t \in [5000, 5200]$ and $t \in [10000, 10200]$. The results are displayed in Fig. S2. One can see that near the maximum point $W^* \simeq 3.6$ and $W^* \simeq 3.7$ for the Heisenberg model with quasiperiodic and

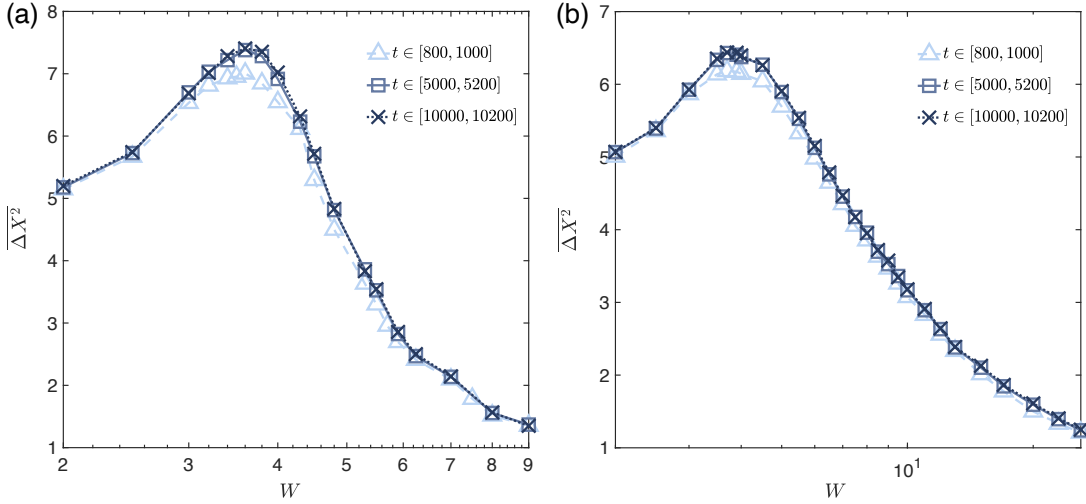


FIG. S2. (a) For the Heisenberg model with quasiperiodic fields with the size $L = 16$, the time-averaged displacement $\overline{\Delta X^2}$ with three different time intervals as a dunction of disorder strength W . (b) is similar to (a) but for the Heisenberg model with random fields.

random potentials, respectively, the $\overline{\Delta X^2}$ becomes slightly larger the time intervals with longer time. Nevertheless, the location of the maximum point of $\overline{\Delta X^2}$ does not substantially change for different time intervals.

In the main text, we perform finite-size scaling analysis based on the data of $\overline{\Delta X^2}$ with $t \in [800, 1000]$. Strictly, the critical point estimated by the data is a finite-time one with $t \simeq 900$. However, as shown in Fig. S2, with the time interval $t \in [800, 1000]$, $\overline{\Delta X^2}$ is quite close to the limit $t \rightarrow \infty$, and does not suffer from strong finite-time effect.

III. DETAILS OF FITTING

In this section, we directly present the fittings of several numerical results in the main text. In Fig. S3(a), we display the fitting of the numerical result shown in Fig. 1(c) of the main text with $L = 22$, taking the logarithmic function $\Delta X^2 \propto \log t$ into consideration. In Fig. S3(b), we display the fitting of the numerical results shown in the inset of Fig. 1(c) of the main text, by using the power-law function $\overline{\Delta X^2} \propto L^\beta$.

For the Floquet model of MBL with $L = 18$, we also fit the dynamics of ΔX^2 by using the logarithmic function [see Fig. S3(c)]. We also employ the power-law function $\overline{\Delta X^2} \propto L^\beta$ to fit the time-averaged ΔX^2 , and the fitting is shown in Fig. S3(d).

IV. DETAILS OF DATA COLLAPSE

The method of performing data collapse is based on Ref. [1]. Finite size scaling has become an fundamental framework for characterizing critical properties of phase transition. A quantity $Q(t, L)$ with scaling depending on two variables, t and L can be expressed as

$$Q(L, t) = L^\lambda f(t \cdot L^{1/\nu}). \quad (\text{S1})$$

Data collapse is a quantitative way to show scaling and determine the exponents and the scaling function $f(x)$ that shows the critical behavior. In this work, we assume that the quantity takes the form of scaling function $Q = \overline{\Delta X^2}(L, W) = L^\lambda g((W - W_c) L^{1/\nu})$. Therefore, the mean residual over all the data points $R = \sum |Q - L^\lambda g((W - W_c) L^{1/\nu})| / N$ (N is the number of data points) reaches minimum for the right choice of (W_c, λ, ν) .

However, we cannot know the exact function form of $g(x)$ with finite known data points. Instead, we estimate the function values using an interpolation scheme, since the function can generally be assumed as an analytic function. Then we can define R^* as

$$R^* = \frac{1}{N} \sum_i \sum_{i \neq j} \sum_n \left| Q_{n,j} - L_j^\lambda \mathcal{G}_i \left((W_{n,j} - W_c) L_j^{1/\nu} \right) \right|, \quad (\text{S2})$$

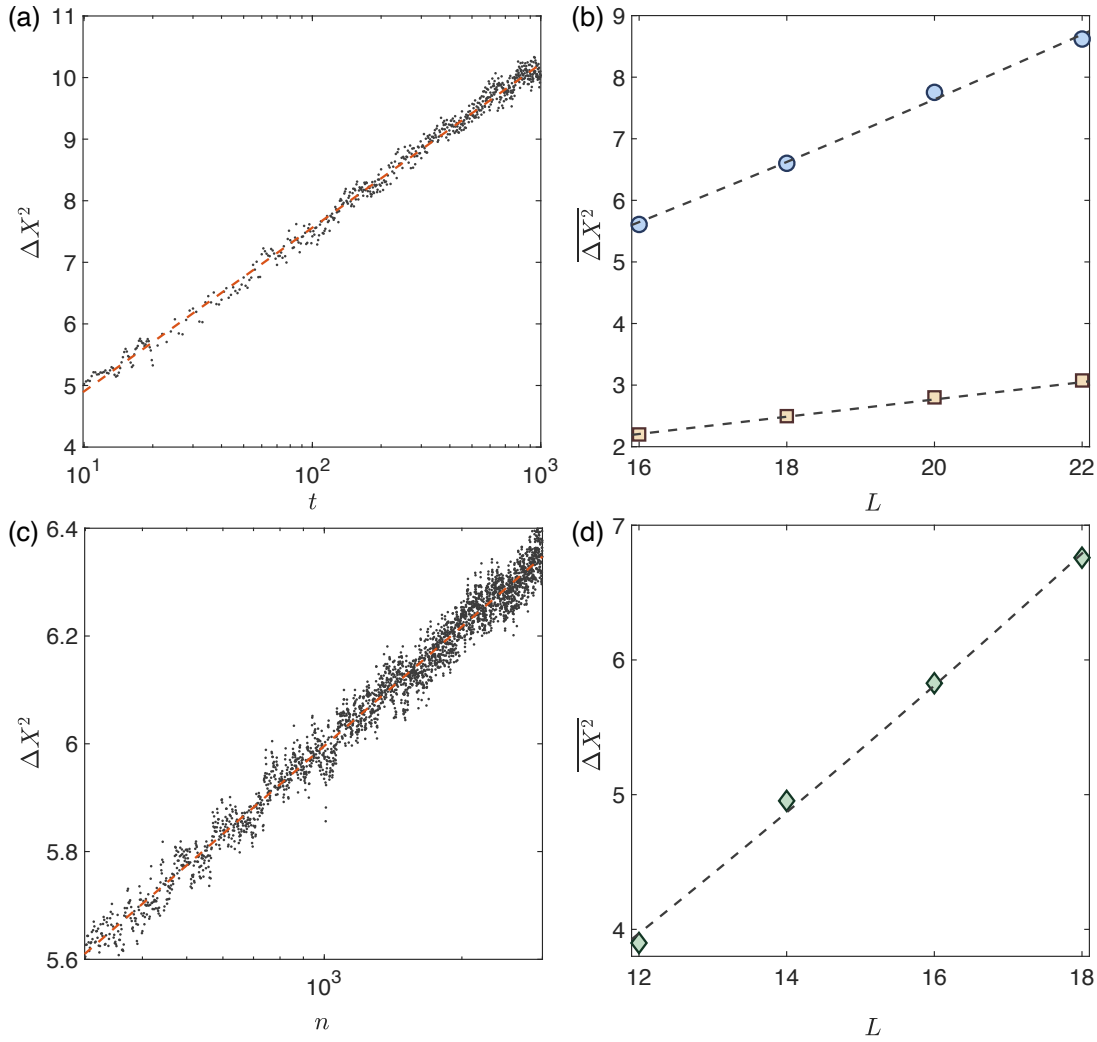


FIG. S3. (a) The logarithmic fit of the dotted numerical data presented in Fig. 1(c) of the main text with $L = 22$ and the time window $t \in [10, 1000]$. (b) The power-law fit of the the numerical data presented in the inset of Fig. 1(c) of the main text. Dashed lines refer to the results of the fittings. (c) The logarithmic fit of the dotted numerical data presented in Fig. 1(f) of the main text with $L = 18$ and the time window $t \in [300, 3000]$. (d) The power-law fit of the the numerical data presented in the inset of Fig. 1(f) of the main text. Dashed lines refer to the results of the fittings. The goodness of fittings in (a)-(d) are larger than 99%.

where $(Q_{n,j}, W_{n,j})$ denotes the n th data point of $\overline{\Delta X^2}$ and the disorder strength W for the system size L_j , and \mathcal{G}_i is the interpolating function based on the data points $(Q_{n,i}, W_{n,i})$ for the system size L_i . Here, we use the linear interpolation for \mathcal{G}_i . An optimization process can then be performed to obtain the minimum value of R^* , determining the values of (W_c, λ, ν) .

For the Heisenberg model with random and quasiperiodic potential, the best data collapse is achieved for the parameters $(W_c, \lambda, \nu) = (6.1, 1.2, 1.4)$ and $(11.7, 1.1, 3.8)$, respectively. For the Floquet model, the parameters obtained from data collapse are $(W_c, \lambda, \nu) = (14.6, 1.1, 3.4)$. In Fig. S4, we plot the value of $\log R^*$ as a function of W and ν , with a fixed value of λ . For the Heisenberg model with random and quasiperiodic potential, we chose $\lambda = 1.2$ and $\lambda = 1.1$, respectively, and for the Floquet model, the chosen value of λ is $\lambda = 1.1$.

Next, we estimate the errors of the data collapse, which can be obtained from the width of the minimum of $\log R^*$. Here, $\log R^*$ is a function of W , ν , and λ , and the minimum point of $\log R^*$ is denoted as $\log R^*(W_c, \nu_0, \lambda_0)$. The width of W_c can be estimated as [1]

$$\Delta W = \eta W_c \left[2 \log \frac{R^*(W_c + \eta W_c, \nu_0, \lambda_0)}{R^*(W_c, \nu_0, \lambda_0)} \right]^{-1/2}. \quad (\text{S3})$$

with $\eta = 1\%$ being a chosen value. Similar to Eq. (S3), the $\Delta \nu$ and $\Delta \lambda$ can also be estimated. For the Heisenberg model with random potential, $\Delta W \simeq 2.0$, $\Delta \nu \simeq 0.5$, and $\Delta \lambda \simeq 0.1$. For the Heisenberg model with quasiperiodic potential, $\Delta W \simeq 0.6$, $\Delta \nu \simeq 0.4$, and $\Delta \lambda \simeq 0.2$. For the Floquet model, $\Delta W \simeq 1.8$, $\Delta \nu \simeq 0.7$, and $\Delta \lambda \simeq 0.1$.

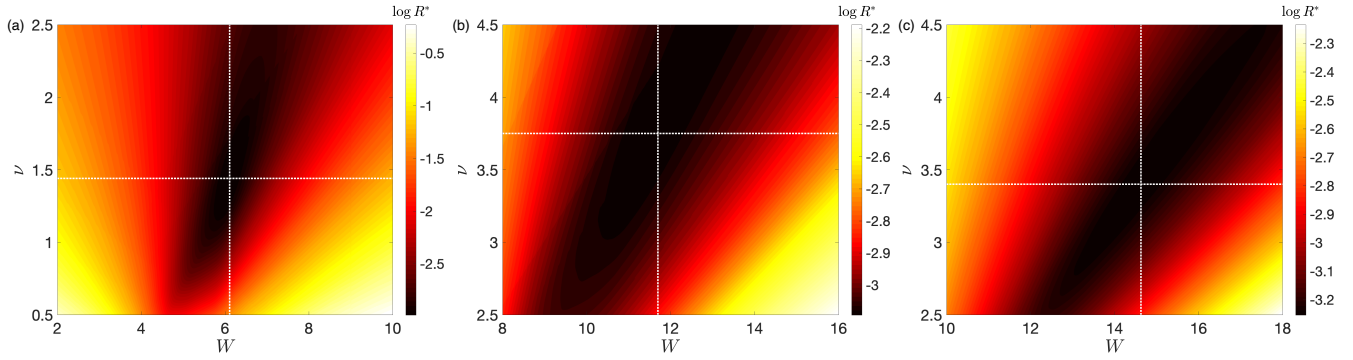


FIG. S4. (a) The value of $\log R^*$ as a function of W and ν for the Heisenberg model with random potential and $\lambda = 1.19$. (b) is similar to (a) but for the Heisenberg model with quasiperiodic potential and $\lambda = 1.09$. (c) The value of $\log R^*$ as a function of W and ν for the Floquet model with $\lambda = 1.11$. The dashed lines represent the values of ν and W with the minimum of $\log R^*$.

V. DYNAMICS OF IMBALANCE IN SYSTEMS WITH LARGER SIZES

In this section, we present the dynamics of imbalance and demonstrate that with the critical points estimated by our method, the imbalance exhibits a freezing dynamics. With the Néel state being the initial state $|\psi_0\rangle$, the imbalance can be defined as

$$I(t) = \frac{n_{\text{odd}} - n_{\text{even}}}{n_{\text{odd}} + n_{\text{even}}} \quad (\text{S4})$$

with

$$n_{\text{odd (even)}} = \frac{1}{L} \langle \psi(t) | \sum_{i \in \text{odd (even)}} (\hat{\sigma}_i^z + \mathbf{1}) | \psi(t) \rangle, \quad (\text{S5})$$

where $\hat{\sigma}_i^z$ is the Z-Pauli matrix, $\mathbf{1}$ is the two-dimensional identity matrix, and $|\psi(t)\rangle = \exp(-i\hat{H}t)|\psi_0\rangle$ is the non-equilibrium state under the unitary evolution of the Hamiltonian \hat{H} . Here, we consider the Hamiltonian \hat{H} of the disordered Heisenberg model with random and quasiperiodic potential studied in the main text.

It has been shown that with an intermediate value of the disorder strength W , the dynamics of imbalance satisfies a power-law decay, i.e., $I(t) \propto t^{-\xi}$, and the freezing of the dynamics of imbalance, i.e., $\xi \simeq 0$ is a key landmark of MBL, from the non-equilibrium perspective [2–8]. We note that numerically, the value of ξ cannot be exactly equal to 0. To estimate the location of critical point via the decay rate ξ , one commonly takes a threshold value ξ_t , which describes the distinguishability between the freezing dynamics and the power-law decay of imbalance. With $\xi \leq \xi_t$, the dynamics of imbalance is freezing and the system lies in the many-body localized phase. For instance, in Ref. [4], the threshold value is chosen as $\xi_t = 0.02$.

In order to demonstrate whether the estimated location of critical points W_c is consistent with the dynamical behaviors of the imbalance, here, we simulate the dynamics of imbalance $I(t)$ for the Heisenberg model with a larger size $L = 50$, by using the time-dependent variational principle (TDVP), as a matrix-product-state-based algorithm [9]. Numerically, we consider the time step size $\delta t = 0.1$ and the bond dimension $\chi = 128$.

For the MBLT in the Heisenberg model with both random and quasiperiodic potential, we consider two estimated values of the critical point. The first one is the critical point estimated in Ref. [10] by using the level spacing ratio, denoted as $W^{(r)}$. The other one is W_c , being the critical point estimated in the main text. For the quasiperiodic model, $W^{(r)} \simeq 4.3$ and $W_c \simeq 6.1$, and for the random model, $W^{(r)} \simeq 5.5$ and $W_c \simeq 11.7$. Figure S5 shows the dynamics of imbalance for the Heisenberg models with the system size $L = 50$, which is simulated by TDVP. It is seen that for both the random and quasiperiodic model, there is an obvious subdiffusive decay of imbalance when $W = W^{(r)}$. In contrast, the decay is suppressed for $W = W_c$, with decay rates in an order of $\xi \simeq 10^{-2}$. In short, taking the freezing dynamics of imbalance as a standard of MBL into consideration, W_c is a better estimation of the critical points of MBLTs than $W^{(r)}$.

-
- [1] Somendra M Bhattacharjee and Flavio Seno, “A measure of data collapse for scaling,” *Journal of Physics A: Mathematical and General* **34**, 6375 (2001).
 [2] Elmer V. H. Doggen, Frank Schindler, Konstantin S. Tikhonov, Alexander D. Mirlin, Titus Neupert, Dmitry G. Polyakov, and Igor V. Gornyi, “Many-body localization and delocalization in large quantum chains,” *Phys. Rev. B* **98**, 174202 (2018).

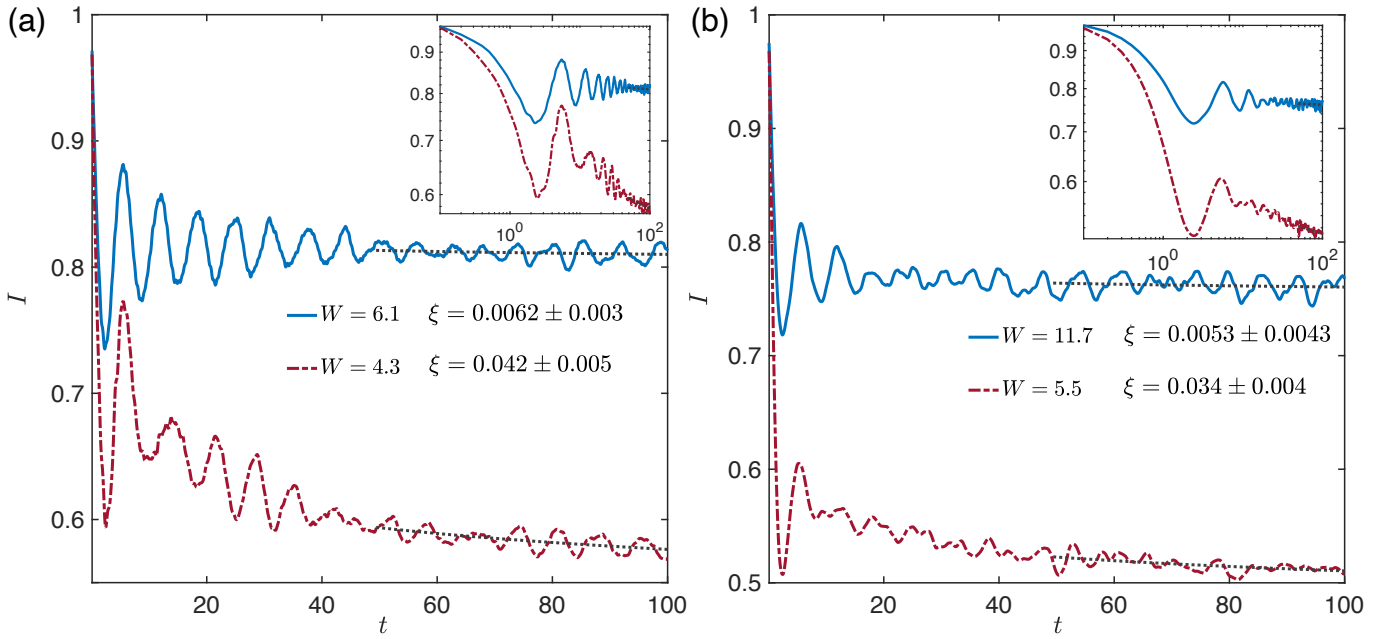


FIG. S5. (a) The dynamics of imbalance for the Heisenberg model with quasiperiodic potential, and different values of disorder strength W . The system size is $L = 50$. The inset shows the same data but in logarithmic axes. (b) is similar to (a) but for the Heisenberg model with random potential. The dotted lines are the fittings of the dynamics of imbalance with the time window $t \in [50, 100]$ by using power-law function $I(t) \propto t^{-\xi}$.

- [3] Elmer V. H. Doggen and Alexander D. Mirlin, “Many-body delocalization dynamics in long Aubry-André quasiperiodic chains,” *Phys. Rev. B* **100**, 104203 (2019).
- [4] Titas Chanda, Piotr Sierant, and Jakub Zakrzewski, “Time dynamics with matrix product states: Many-body localization transition of large systems revisited,” *Phys. Rev. B* **101**, 035148 (2020).
- [5] Piotr Sierant and Jakub Zakrzewski, “Challenges to observation of many-body localization,” *Phys. Rev. B* **105**, 224203 (2022).
- [6] Henrik P. Lüschen, Pranjal Bordia, Sebastian Scherg, Fabien Alet, Ehud Altman, Ulrich Schneider, and Immanuel Bloch, “Observation of slow dynamics near the many-body localization transition in one-dimensional quasiperiodic systems,” *Phys. Rev. Lett.* **119**, 260401 (2017).
- [7] Pranjal Bordia, Henrik Lüschen, Sebastian Scherg, Sarang Gopalakrishnan, Michael Knap, Ulrich Schneider, and Immanuel Bloch, “Probing slow relaxation and many-body localization in two-dimensional quasiperiodic systems,” *Phys. Rev. X* **7**, 041047 (2017).
- [8] Elmer V. H. Doggen, Igor V. Gornyi, Alexander D. Mirlin, and Dmitry G. Polyakov, “Slow many-body delocalization beyond one dimension,” *Phys. Rev. Lett.* **125**, 155701 (2020).
- [9] Jutho Haegeman, Christian Lubich, Ivan Oseledets, Bart Vandereycken, and Frank Verstraete, “Unifying time evolution and optimization with matrix product states,” *Phys. Rev. B* **94**, 165116 (2016).
- [10] Vedika Khemani, D. N. Sheng, and David A. Huse, “Two universality classes for the many-body localization transition,” *Phys. Rev. Lett.* **119**, 075702 (2017).